RESEARCH ARTICLE





Geochronological constraints on Caledonian strike-slip displacement in Svalbard, with implications for the evolution of the Arctic

Karol Faehnrich^{1,2} | Jarosław Majka^{2,3} | David Schneider⁴ | Stanisław Mazur⁵ | Maciej Manecki² | Grzegorz Ziemniak² | Virginia T. Wala¹ | Justin V. Strauss¹

Correspondence

Karol Faehnrich, Department of Earth Sciences, Dartmouth College, Hanover, NH, LISA

Email: karol.faehnrich.gr@dartmouth.edu

Funding information

National Science Centre, Poland, Grant/ Award Number: 2015/17B/ST10/03114; National Science Foundation, Division of Earth Sciences, Grant/Award Number: EAR-1650152; AGH - University of Science and Technology, Grant/Award Number: 11.11.14 0.158

Abstract

The timing of Svalbard's assembly in relation to the mid-Paleozoic Caledonian collision between Baltica and Laurentia remains contentious. The Svalbard archipelago consists of three basement provinces bounded by N–S-trending strike–slip faults whose displacement histories are poorly understood. Here, we report microstructural and mineral chemistry data integrated with ⁴⁰Ar/³⁹Ar muscovite geochronology from the sinistral Vimsodden-Kosibapasset Shear Zone (VKSZ, southwest Svalbard) and explore its relationship to adjacent structures and regional deformation within the circum-Arctic. Our results indicate that strike–slip displacement along the VKSZ occurred in late Silurian–Early Devonian and was contemporaneous with the beginning of the main phase of continental collision in Greenland and Scandinavia and the onset of syn-orogenic sedimentation in Silurian–Devonian fault-controlled basins in northern Svalbard. These new-age constraints highlight possible links between escape tectonics in the Caledonian orogen and mid-Paleozoic terrane transfer across the northern margin of Laurentia.

1 | INTRODUCTION

Strike-slip deformation plays a significant role in the evolution of convergent plate margins (Teyssier, Tikoff, & Markley, 1995; Woodcock, 1986). However, due to fault reactivation and/or burial beneath successor basins, documenting ancient strike-slip displacement is challenging and controversial. One example of an oblique collisional orogen with evidence for widespread strike-slip displacement is the Caledonides (Figure 1a; Harland & Wright, 1979). The Caledonian orogen represent one of the most significant collisional events of the Paleozoic Era, resulting in the closure of the northern lapetus Ocean (e.g. Dewey & Strachan, 2003; Gee, 1975; Soper, Strachan, Holdsworth, Gayer, & Greiling, 1992), subduction of

Baltica beneath Laurentia to depths >100 km (e.g. Gee, Majka, Janák, Robinson, & Roermund, 2013) and the potential initiation of a west-ward-propagating Scotian-style subduction zone that facilitated the dispersal of peri-Baltic and peri-Laurentian terranes into the North American Cordillera (Northwest Passage of Colpron & Nelson, 2009; Miller et al., 2011; Strauss et al., 2017; Strauss, Macdonald, Taylor, Repetski, & McClelland, 2013). Despite this, there remains significant ambiguity regarding the kinematics and tectono-thermal history of the northern Caledonides in relation to the tectonic evolution of the circum-Arctic.

The Svalbard archipelago hosts an array of N-S trending Caledonian strike-slip faults that separate pre-Devonian basement into the Northeastern, Northwestern and Southwestern Basement

290 © 2020 John Wiley & Sons Ltd wileyonlinelibrary.com/journal/ter Terra Nova. 2020;32:290–299.

¹Department of Earth Sciences, Dartmouth College, Hanover, NH, USA

²Faculty of Geology, Geophysics and Environment Protection, AGH – University of Science and Technology, Kraków, Poland

³Department of Earth Sciences, Uppsala University, Uppsala, Sweden

⁴Department of Earth and Environmental Sciences, University of Ottawa, Ottawa, ON, Canada

⁵Institute of Geological Sciences, Polish Academy of Sciences, Kraków, Poland

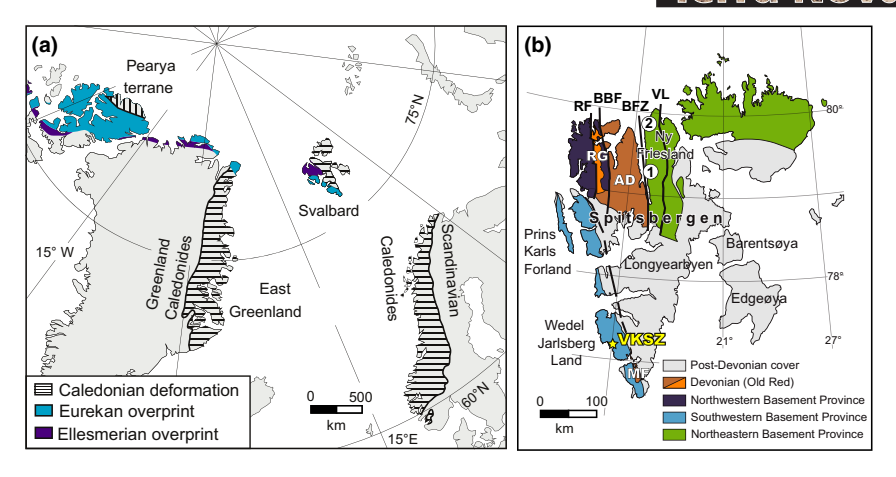


FIGURE 1 (a) Schematic map showing location of Svalbard archipelago and extent of Caledonian, Ellesmerian and Eurekan deformation from McClelland, Von Gosen, and Piepjohn (2019). (b) Simplified geologic map of the Svalbard archipelago. Svalbard is composed of three basement provinces separated by N–S- to NW–SE-trending fault zones. Radiometric ages referred to in the text include: (1) ca. 410 Ma U–Pb titanite age from Johansson et al. (1995), (2) ca. 420 Ma ⁴⁰Ar/³⁹Ar hornblende and muscovite ages of Gee and Page (1994). Abbreviations: RF–Raudfjorden Fault, BBF–Breibogen-Bockfjorden Fault, BFZ–Billefjorden Fault Zone, VL–Veteranen Line, AD–Andreeland-Dicksonland Graben, RG–Red Bay Group, MF–Marietoppen Formation, VKSZ–Vimsodden-Kosibapasset Shear Zone (modified from Gee & Tebenkov, 2004, basement province nomenclature after Dallmann, Elvevold, Majka, & Piepjohn, 2015) [Colour figure can be viewed at wileyonlinelibrary.com]

provinces (SBP; Figure 1b, Dallmann et al., 2015; Gee & Page, 1994; Gee & Tebenkov, 2004 see also Harland, Scott, Aukland, & Snape, 1992). Strike-slip deformation in Svalbard has been linked to the peak Scandian phase of Caledonian collision (c. 430-400 Ma, e.g. Gee & Page, 1994); critically, however, other models for Svalbard's assembly postulate pre- and post-Scandian strike-slip displacement (Gasser & Andresen, 2013; Harland et al., 1992; Michalski, Lewandowski, & Manby, 2012; Ohta, Dallmeyer, & Peucat, 1989) and others invoke extension related to orogenic collapse (Braathen, Osmundsen, Maher, & Ganerød, 2018). These contrasting tectonic models emphasize important ambiguities in our understanding of the tectonic history of the North Atlantic and circum-Arctic regions (e.g. Pease, 2011) and potential relationships among crustal thickening, tectonic escape and terrane transfer in collisional orogens (e.g. Gee & Page, 1994; Molnar & Tapponier, 1975; Ohta, 1994; Tapponier, Peltzer, Le Dain, Armijo, & Cobbold, 1982). To provide critical new tectono-thermal constraints on the assembly of Svalbard and its relationship to the evolution of the circum-Arctic, we integrate previous thermochronological work with new microstructural analyses, mineral chemistry data and multiple single-grain fusion 40Ar/39Ar muscovite geochronological results from sinistral shear zones in south-western Svalbard.

2 | GEOLOGICAL BACKGROUND

Despite their regional significance, the age and kinematics of Svalbard's major structural boundaries are still poorly constrained. In the Northeastern Basement Province, evidence for late Silurian to Early Devonian transpression and strike-slip displacement is represented by *c.* 420–410 Ma ⁴⁰Ar/³⁹Ar muscovite

(Gee & Page, 1994) and *c.* 410 Ma U-Pb titanite ages (Johansson, Gee, Björklund, & Witt-Nilsson, 1995). This strike-slip deformation is supported by the onset of syn-orogenic sedimentation in presumed transtensional basins of north-central Svalbard (Friend, Harland, Rogers, Snape, & Thornley, 1997; Gee & Moody-Stuart, 1966; McCann, 2000). In contrast, mylonites exposed along the sinistral Billefjorden Fault Zone (BFZ, Figure 1b; Harland et al., 1974) separating the Northeastern Basement Province and clastic Devonian strata, more recently yielded *c.* 450 Ma ⁴⁰Ar/³⁹Ar muscovite ages, which have been proposed as evidence for pre-Scandian basement assembly (Michalski et al., 2012). Late Devonian, or post-Scandian, displacement along the BFZ and other strike-slip fault systems in northern Svalbard was also proposed based on regional stratigraphic correlations (e.g. Harland et al., 1992; Harland & Wright, 1979).

Within southern Wedel Jarlsberg Land (WJL) of the SBP, Mazur et al. (2009) documented crustal fragments of different metamorphic grade and origin separated by a major strike-slip fault system called the Vimsodden-Kosibapasset Shear Zone (VKSZ; Figure 2). Although not the major bounding structure of the SBP, the VKSZ does represent a profound crustal boundary with clear sinistral kinematic indicators (Mazur et al., 2009); Majka et al. (2015) proposed a northern continuation of this structure to juxtapose amphibolite facies rocks of the Berzeliuseggene Unit in northern WJL and the Isbjørnhamna Group and Eimfjellet Complex in southern WJL with low-grade Neoproterozoic metasedimentary rocks of the Deilegga and Sofiebogen groups (Figure 2). The former higher grade units were metamorphosed c. 640 Ma (Torellian event, Majka et al., 2014, 2015) and show an affinity to the Timanide orogen of Baltica, whereas the lower-grade rocks share similarities to the Pearya terrane of northern Ellesmere Island, Canada (Majka et al., 2014).

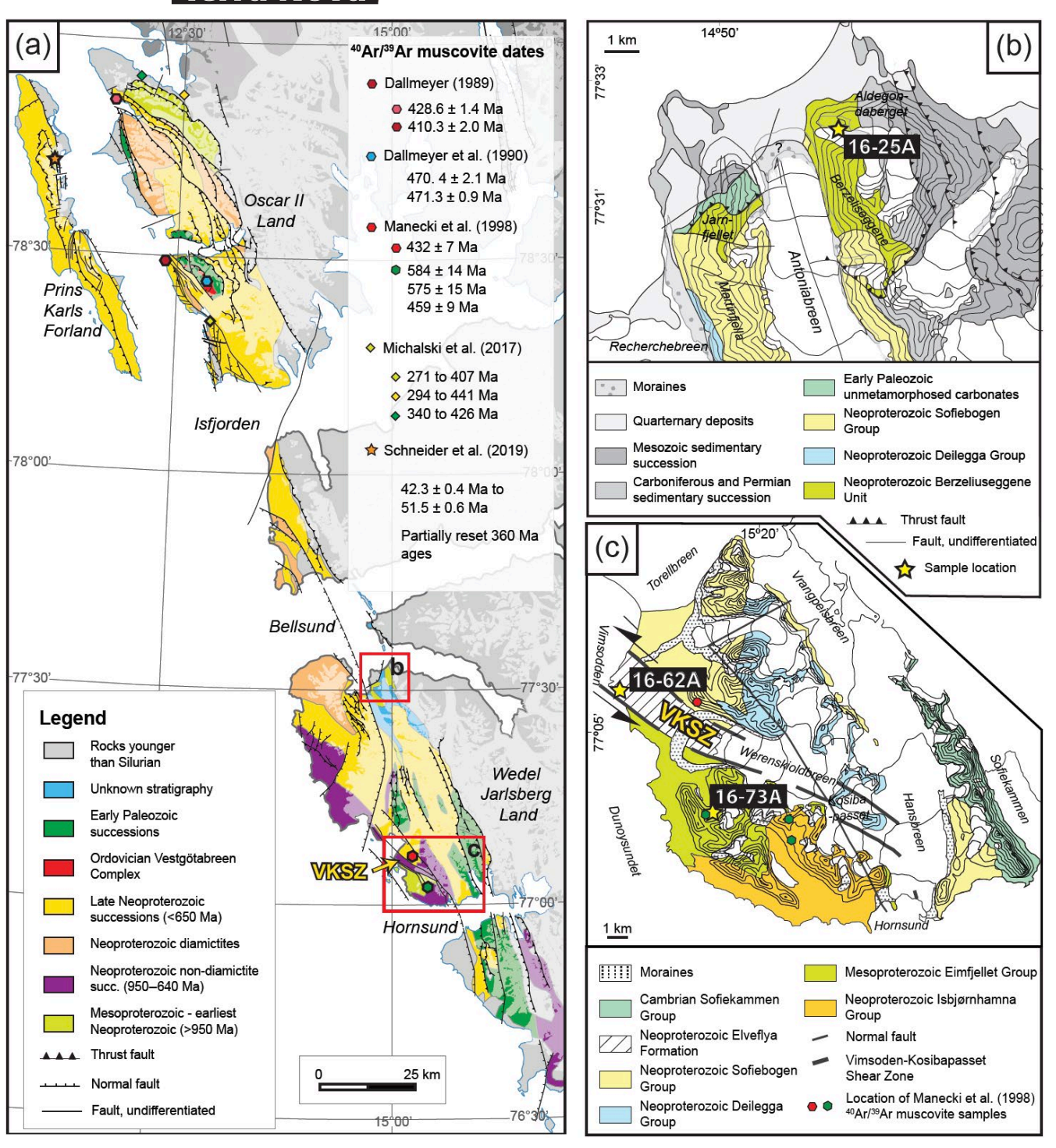


FIGURE 2 (a) Simplified geologic map of the Southwestern Basement Province modified from Dallmann et al. (2015). Locations for samples with published muscovite ⁴⁰Ar/³⁹Ar ages are marked on the map. Results from Dallmeyer (1989), Dallmeyer et al. (1990) and Manecki, Holm, Czerny, and Lux (1998) are step-heating plateau ages, whereas dates in Michalski et al. (2017) were obtained by UV laser ablation analysis and Schneider et al. (2019) by total fusion analysis. Results of K-Ar and ⁴⁰Ar/³⁹Ar dating of other minerals are not included (summarized in Majka & Kośmińska, 2017). (b) Simplified geologic map of the Bellsund area with exposures of the Berzeliuseggene Unit modified from Majka et al. (2015). (c) Simplified geologic map of the Vimsodden area modified from Mazur et al. (2009). Coordinates for sampling locations: 16-25A (77.53853°N, 14.94522°E); 16-62A (77.10822°N, 15.04183°E) and 16-73A (77.04743°N, 15.21800°E) [Colour figure can be viewed at wileyonlinelibrary.com]

 40 Ar/ 39 Ar muscovite ages from the SBP reflect a protracted tectono-thermal history generally interpreted as evidence for widespread *c.* 430–400 Ma Caledonian metamorphism (Dallmeyer,

1989, Manecki et al., 1998) that overprinted late Neoproterozoic metamorphism (c. 640 Ma) in WJL (Majka et al., 2014; Majka, Mazur, Manecki, Czerny, & Holm, 2008; Manecki et al., 1998) and Middle

Ordovician metamorphism (c. 470 Ma) in Oscar II Land (Dallmeyer, Peucat, Hirajima, & Ohta, 1990; Labrousse, Elvevold, Lepvrier, & Agard, 2008). These metamorphic events are further overprinted by Paleocene–Eocene Eurekan deformation (Figure 1a; Dallmeyer, 1989; Michalski, Manby, Nejbert, Domańska-Siuda, & Burzyński, 2017; Schneider, Faehnrich, Majka, & Manecki, 2019), which significantly hinders local interpretations of ⁴⁰Ar/³⁹Ar data; thus, despite decades of work on key tectonic boundaries in south-western Svalbard (e.g. Dallmann et al., 2015; Harland, 1997), the temporal history of basement juxtapositon remains speculative (Mazur et al., 2009).

3 | RESULTS

3.1 | Petrographic and Microstructural Analyses

Twenty-nine samples from prominent shear zones in northern and southern WJL were collected to better resolve the timing of displacement along a gradient towards the VKSZ (Figure 2). Petrographic thin sections were examined, and three representative

samples that show evidence for growth of muscovite larger than 100 μm during deformation were chosen for $^{40} Ar/^{39} Ar$ muscovite geochronology. Sample 16-25A was collected on the southern slope of Aldegondaberget (Figure 2b) and consists of a muscovite schist of the Berzeliuseggene Unit with mineral stretching lineation plunging to the north (359/29; Figure 3a). Sample 16-62A was collected from the Elveflya Formation (Czerny, Kieres, Manecki, & Rajchel, 1993) within the central zone of the VKSZ (Figure 2c) and is a highly sheared matrix-supported conglomerate with sparse elongated clasts of quartzite and dolostone (Figure 3c). Sample 16-73A was collected just south of the VKSZ at Bratteggdalen (Figure 2c) from the Mesoproterozoic Eimfjellet Complex (Czerny et al., 1993) and is a mica schist from a zone of deformation trending subparallel to the VKSZ (Figure 3e).

The samples all show clear evidence for (re)crystallization of muscovite and quartz during deformation (Figure 3). Sample 16-25A has two populations of muscovite that can be distinguished based on their size and microstructural position. The first population of muscovite (Ms-I) forms 100–500 μ m mica fish, which are overgrown by a second generation of muscovite (Ms-II) that forms bundles and needles aligned within the foliation planes

FIGURE 3 Field photographs and photomicrographs of samples investigated in this study. (a) Sample 16-25A is muscovite schist occurring within augen gneiss on the north-western slopes of Aldegondaberget ridge. Hammer for scale is 32 cm long. (b) Mica fish (Ms-I) overgrown by muscovite (Ms-II) in the form of needles and bundles. (c) Sample 16-62A consists of a highly sheared matrix-supported conglomerate within the Vimsodden-Kosibapasset Shear Zone (VKSZ). Hammer for scale is 32 cm long. (d) Muscovite occurs as elongated ribbons that are internally deformed by C'-type shear bands. (e) Sample 16-73A comes from a localized shear zone within the Eimfjellet Group that trends subparallel to the VKSZ. Hammer for scale is 32 cm long. (f) Interconnected mica layers in sample 16-73A are internally deformed by C'-type shear bands, quartz is dynamically recrystallized through grain boundary migration. Abbreviations: Qz, quartz; Ms, muscovite; Pl, plagioclase [Colour figure can be viewed at wileyonlinelibrary.com]

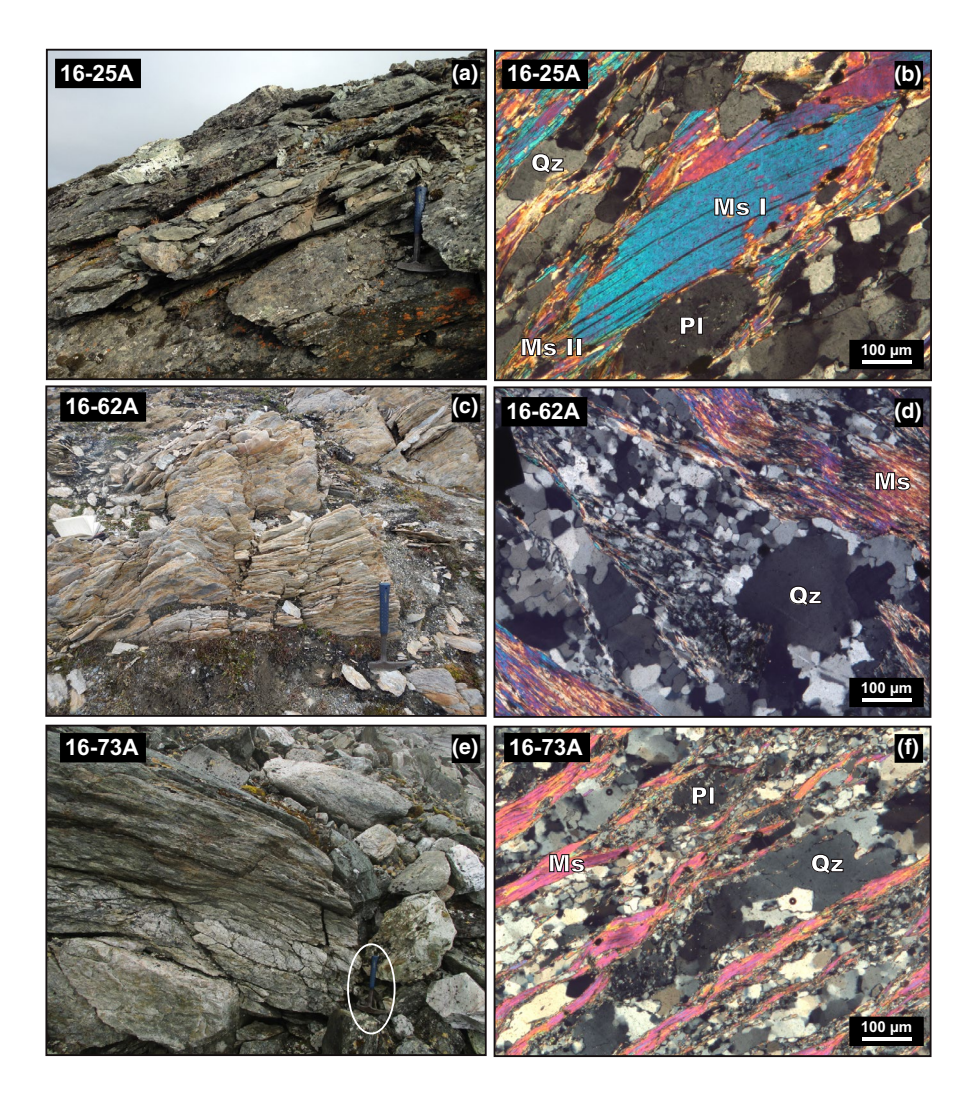


(Figure 3b). Both populations of muscovite occur in layers between dynamically recrystallized quartz bearing evidence for grain boundary migration (Figure 3b). In sample 16-62A, muscovite forms anastomosing ribbons and interconnected bundles up to 300 μm , which are affected by C'-type shear bands (Figure 3d). Similarly, in sample 16-73A, muscovite forms interconnected ribbons up to 100 μm that are internally deformed by C'-type shear zones. In both samples 16-62A and 16-73A, grain boundary migration is a dominant mechanism for quartz recrystallization (Figure 3f).

3.2 | Muscovite geochemistry

In addition to contrasting microstructural position and morphology, the two muscovite populations in sample 16-25A differ in their geochemistry (Figure 4, Table S1). Ms-I forms chemically zoned mica fish with sharp internal boundaries between core and rim (Figure 4) with Si increasing from 3.1 to 3.3 atoms per formula unit (a.p.f.u.), whereas data from Ms-II form a homogenous population with Si values ranging from 3.11 to 3.15 a.p.f.u. and lower Ti content than in Ms-I (Figure 5).

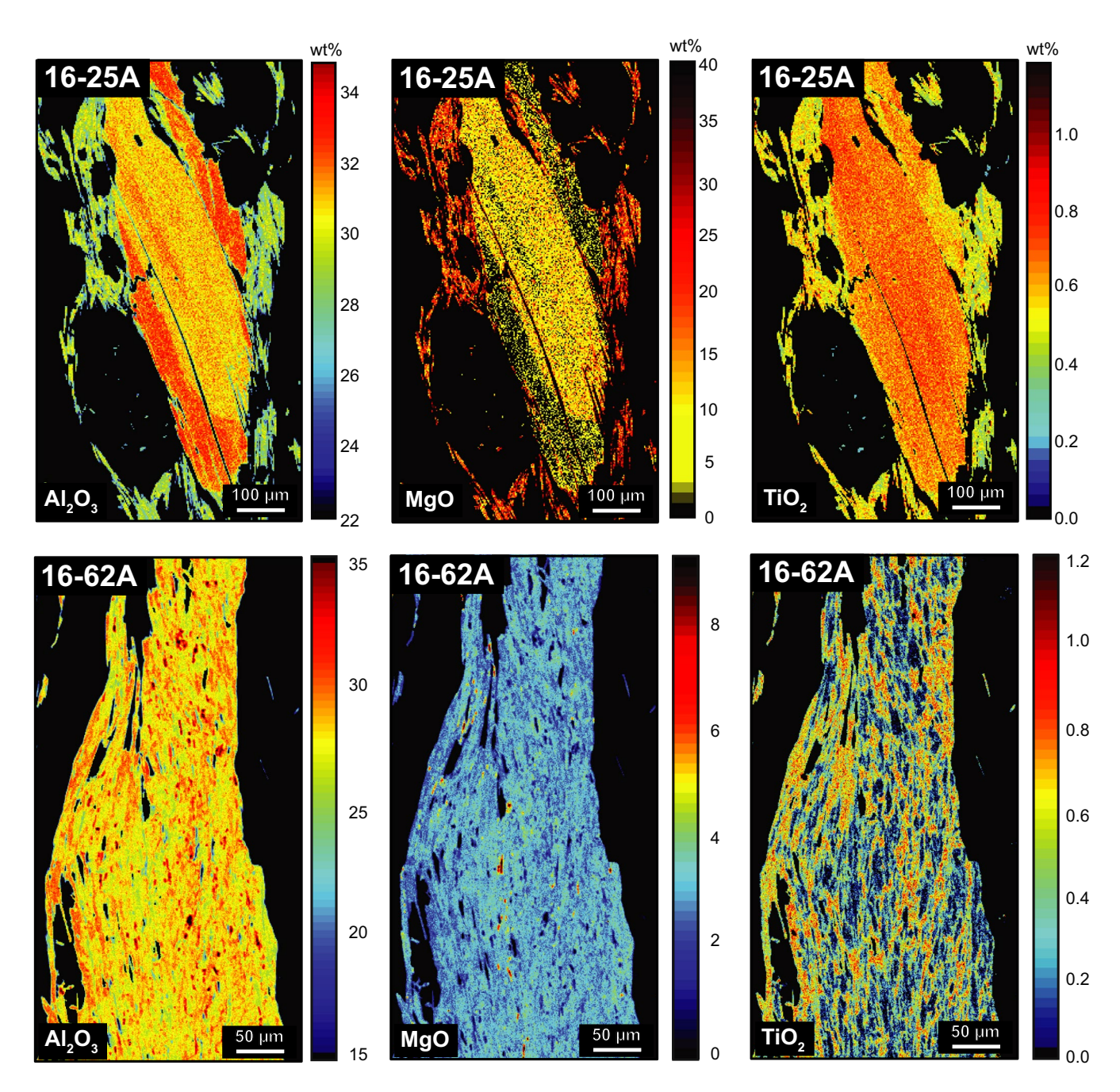


FIGURE 4 X-ray chemical maps of muscovite showing variation in Al_2O_3 , MgO and TiO_2 concentrations. Sample 16-25A has two generations of mica: Ms-II has lower Al_2O_3 and TiO_2 and higher MgO contents with respect to Ms-I (mica fish). Ms-I also displays internal chemical variations with higher values of Al in the rim. Sample 16-62A is relatively homogenous with respect to the distribution of Al_2O_3 and MgO. All of the maps were processed in XmapTools (Lanari et al., 2014) [Colour figure can be viewed at wileyonlinelibrary.com]

FIGURE 5 Results of electron microprobe analyses of muscovite. (a) K-bearing white mica octahedral site (Fe + Mg) occupancy (corrected for the di/trioctahedral substitution) versus Si content. The line corresponds to the Tschermak substitution after Parra, Vidal, and Agard (2002). (b) A binary plot of Ti versus Al content. Abbreviations: Acel, Alceladonite; Ms, muscovite [Colour figure can be viewed at wileyonlinelibrary.com]

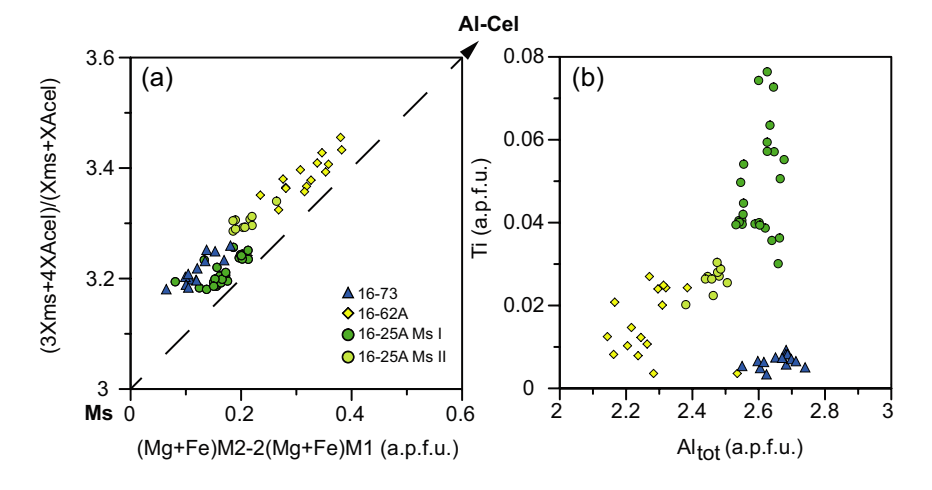
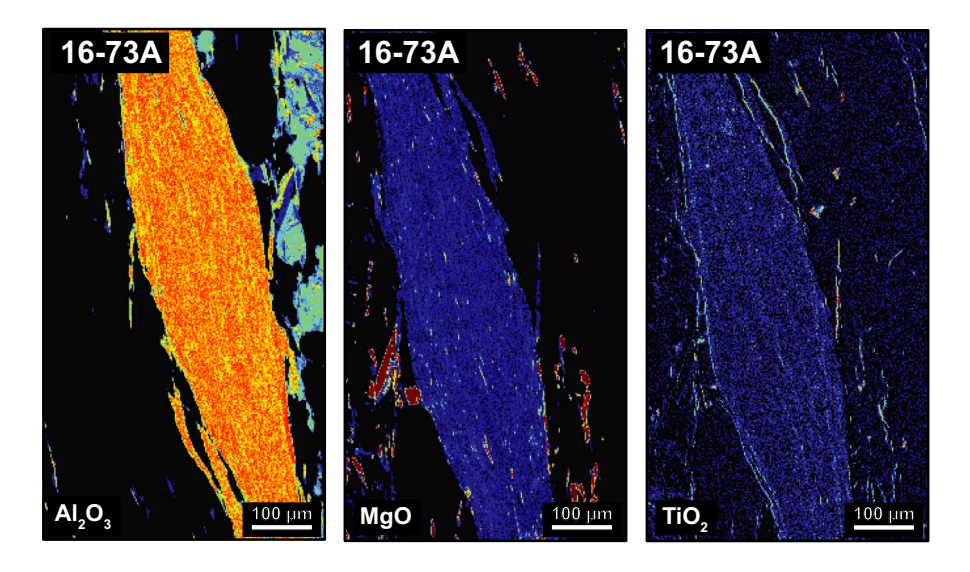


FIGURE 6 X-ray chemical maps of muscovite showing variation in Al₂O₃, MgO and TiO₂ content from sample 16-73A. Warm colours are higher elemental concentrations and cooler colours indicate lower elemental concentrations. The muscovite is homogenous, indicating one stage of growth or complete recrystallization during deformation. Maps processed in ImageJ [Colour figure can be viewed at wileyonlinelibrary.com]



In sample 16-62A, only one population of muscovite is distinguished with no clear zonation other than a patchy distribution of Ti and Al (Figure 4). The muscovite has a relatively high value of Si (increasing from 3.12 to 3.24 a.p.f.u.) and octahedral site occupancy (Figure 5a) with low Ti content (Figure 5b). Similarly, sample 16-73A shows only one population of muscovite (Figure 6), but it has a significantly different chemical composition (Figure 5a) with much lower Ti values (up to 0.01 a.p.f.u) than in sample 16-25A (Figure 5b).

3.3 | ⁴⁰Ar/³⁹Ar Muscovite Geochronology

Whole rock samples for $^{40}\text{Ar}/^{39}\text{Ar}$ geochronology were hand crushed with a mortar and pestle and sieved to concentrate ~106–250 μm muscovite grains. These crystals were picked under a binocular microscope, but specific grain morphologies were not targeted. Seven to eight muscovite grains were analysed per sample via total fusion $^{40}\text{Ar}/^{39}\text{Ar}$ geochronology at the University of Manitoba (Winnipeg, Canada) using a multi-collector Thermo Fisher Scientific ARGUS VI mass spectrometer, linked to a stainless steel Thermo Fisher

Scientific extraction/purification line and Photon Machines (55 W) Fusions 10.6 $\rm CO_2$ laser (Figure 7 and Table S2).

The calculated dates from the Berzeliuseggene Unit (16-25A) vary from 599.8 \pm 19.4 Ma to 410.2 \pm 17.6 Ma with a main population at 548 \pm 14 Ma (weighted average, n = 6). Less dispersed data were noted in sheared conglomerate from the VKSZ (16-62A), where muscovite produced dates ranging from 434.1 \pm 3 Ma to 400.7 \pm 15.8 Ma and a weighted average of 424 \pm 6 Ma (n = 8). Finally, muscovite from the Eimfjellet Complex (16-73A) produced dates in the range of 537.9 \pm 21 Ma to 443.1 \pm 10.1 Ma with a weighted average of 462 \pm 11 Ma (calculated from Ordovician dates, n = 6).

4 | DISCUSSION

4.1 | Cooling versus (re)crystallization

Samples from the SBP presented herein contain microstructural and geochemical evidence for (re)crystallization of muscovite during deformation, with quartz dynamically recrystallized through grain boundary migration (Figure 3). The microstructural observations

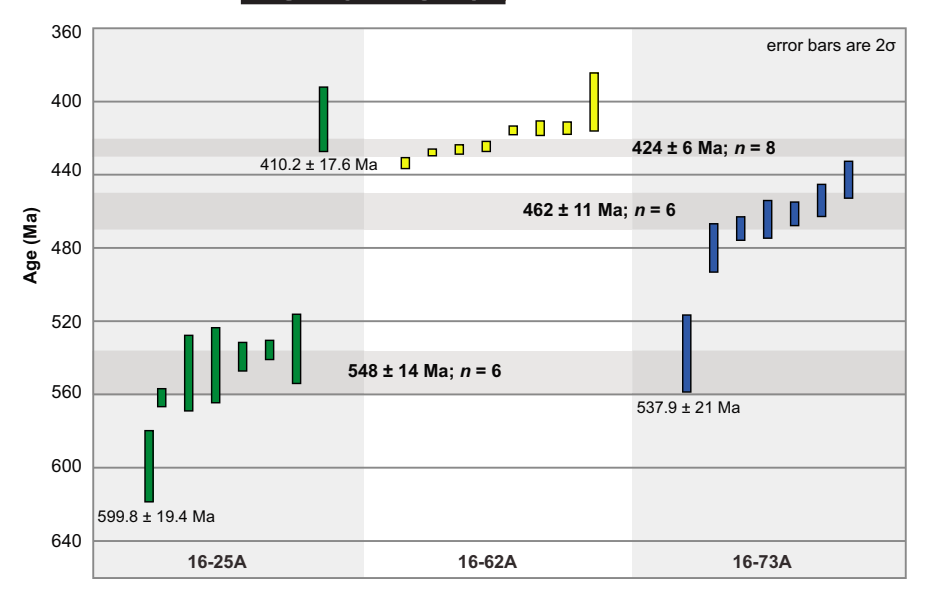


FIGURE 7 Composite 40Ar/39Ar weighted average plot from samples 16-25A, 16-62A and 16-73A. Each vertical bar represents a single age reported at 2σ. Dates from the Berzeliuseggene Unit (sample 16-25A) vary from 599.8 ± 19.4 Ma to 410.2 ± 17.6 Ma with the main population around 548 ± 14 Ma (n: 6). Sample 16-62A produced less age dispersal with a range from 434.1 ± 3 Ma to 400.7 ± 15.8 Ma (weighted average of 424 ± 6 Ma). Data from the Eimfiellet Group (sample 16-73A) range from 537.9 ± 21 Ma to 443.1 ± 10.1 Ma with a weighted average of 462 ± 11 Ma (n: 6) [Colour figure can be viewed at wileyonlinelibrary.com]

suggest deformation temperatures in the range of 400-500°C (Mancktelow & Pennacchioni, 2004; Stipp, Stünitz, Heilbronner, & Schmid, 2002; Urai, Means, & Lister, 1986; Vidal, Kubin, Debat, & Soula, 1980) within the uppermost part of the nominal muscovite ⁴⁰Ar* closure temperature window (Dodson, 1973; Dunlap, 1997; Harrison, Célérier, Aikman, Hermann, & Heizler, 2009). We propose the older dates (599.8 ± 19.4 Ma to 535.3 ± 18.9 Ma) in sample 16-25A represent Ms-I (Figures 3 and 4) and interpret these as mixed ages from initial growth during c. 640 Ma metamorphism (Majka et al., 2015) and partial resetting during Caledonian metamorphism. We hypothesize that the 410 \pm 18 Ma 40 Ar/ 39 Ar date represents (re) crystallization of the metamorphic Ms-II during greenschist facies metamorphism, which is supported by high Si and low Ti values in muscovite with the removal of Ar* (Mulch & Cosca, 2004). We speculate that due to the small size of Ms-II (~100 μm) and our targeted grain size between ~106 and 250 µm, more of this muscovite age population was not captured.

In sample 16-62A, the single age population with a weighted average of 424 \pm 6 Ma corresponds to a chemically homogenous population that grew during sinistral ductile deformation in temperatures slightly above the $^{40}\mathrm{Ar}^*$ closure temperature for muscovite. This date most likely reflects rapid cooling after deformation, which is also supported by undisturbed 432 \pm 7 Ma $^{40}\mathrm{Ar}/^{39}\mathrm{Ar}$ plateau ages from samples in the Sofiebogen Group just north of the VKSZ (Manecki et al., 1998), which were previously interpreted as the timing of greenschist facies metamorphism. We interpret the 424 \pm 6 Ma weighted average age as the most likely approximation for the timing of sinistral strike–slip displacement along the VKSZ.

Finally, sample 16-73A produced a population of muscovite with 40 Ar/ 39 Ar dates of c. 462 ± 11 Ma, along with inheritance of a single 538 ± 21 Ma grain. The Cambrian date most likely reflects partial to complete recrystallization of c. 640 Ma metamorphic muscovite, a potential remnant of the amphibolite facies Torrelian metamorphism documented in the adjacent

Isbjørnhamna Group (Majka et al., 2008). We propose the mica recrystallization occurred either during *c*. 460 Ma metamorphism, as suggested by the dominant age population and the fact that Ordovician metamorphic rocks occur locally within the SBP (e.g. Dallmann et al., 2015), or during greenschist facies metamorphism at *c*. 420–430 Ma as recorded in the adjacent Sofiebogen Group (Manecki et al., 1998). Overall, our results from samples just south and north of the VKSZ show evidence for partial resetting of older grains, but there is complete (re)crystallization within the VKSZ, which we interpret as the most likely timing for strike–slip displacement along this major shear zone.

4.2 | Tectonic implications

Our geochronological results from the SBP provide evidence for late Silurian-Early Devonian strike-slip deformation in Svalbard and suggest displacement within the VKSZ was synchronous with Scandian deformation in the Caledonides. Continuation of the VKSZ as a part of a larger anastomosing system of Caledonian shear zones along the eastern boundary of the SBP (Majka et al., 2015) is supported herein by the single 410.2 ± 17.6 Ma age from the Berzeliuseggene Unit. Published ⁴⁰Ar/³⁹Ar ages from Oscar II Land highlight a more regional c. 420 Ma tectono-thermal event in the SBP (Dallmeyer, 1989; Dallmeyer et al., 1990), which may be further substantiated by the c. 420-410 Ma 40 Ar/ 39 Ar and U-Pb ages from shear zones within the Northeastern Basement Province (Gee & Page, 1994; Johansson et al., 1995). Thus, our geochronological data indicate that strike-slip displacement occurred in both north-eastern and south-western Svalbard at the same time, which broadly supports models for late Silurian-Early Devonian amalgamation of Svalbard as far-field products of the Scandian collision (Gee & Page, 1994). The c. 450 Ma ⁴⁰Ar/³⁹Ar muscovite ages from the BFZ may not necessarily reflect the timing of strike-slip displacement, but rather could indicate partial resetting of earlier

metamorphic ages (the reported dates range from 468 ± 5 Ma to 436 ± 2 Ma, Michalski et al., 2012) or cooling after Ordovician deformation and metamorphism.

The timing of strike-slip displacement along the VKSZ is broadly synchronous with the onset of "Old Red" syn-orogenic sedimentation in northern and southern Svalbard, as well as the greater circum-Arctic (Friend et al., 1997); thus, in contrast to models of widespread extensional collapse (Braathen et al., 2018), active late Silurian-Early Devonian strike-slip faults across the major structural boundaries of Svalbard's basement provinces may have controlled the onset of syn-orogenic sedimentation in Svalbard and the North Atlantic, although this strike-slip displacement does not preclude the presence of local extensional detachments in northern Svalbard. In our view, the prominent system of late Silurian-Early Devonian shear zones and synorogenic deposits exposed along the western edge of Svalbard may reflect key terrane-bounding sinistral shear zones (e.g., McClelland, Malone, Gosen, Piepjohn, & Laeufer, 2012) and transtensional basins (McCann, 2000) that are characteristic features of the Arctic margin of Laurentia and a fundamental requirement of the Northwest Passage model for mid-Paleozoic terrane displacement along the northern margin of Laurentia (Colpron & Nelson, 2009). Together, these data highlight orogen-scale linkages among contraction, distal tectonic escape and terrane fragmentation, highlighting the importance of strike-slip systems in contractional orogens.

ACKNOWLEDGEMENTS

We thank Jerzy Czerny for his support in the field and discussions about regional geology, Piotr Zagórski and the research team of Calypsobyen for hospitality, the Polish Polar Station in Hornsund for logistical support and Adam Włodek for assistance with EMP analyses. This research was supported by the National Science Centre (Poland) research project no. 2015/17B/ST10/03114 (JM) and the National Science Foundation (USA) Tectonics Grant EAR-1650152 (JVS). MM was partly funded from AGH University of Science and Technology, Poland, research project no 11.11.140.158. We thank three anonymous Reviewers, Associate Editor and Science Editor Klaus Mezger for helpful feedback that helped improve the manuscript and editorial support.

DATA AVAILABILITY STATEMENT

The authors confirm that the data supporting the findings of this study are available within the article and its supplementary materials.

ORCID

Karol Faehnrich https://orcid.org/0000-0001-7052-2494

Jarosław Majka https://orcid.org/0000-0002-6792-6866

David Schneider https://orcid.org/0000-0002-9665-4927

Stanisław Mazur https://orcid.org/0000-0002-6560-1048

Maciej Manecki https://orcid.org/0000-0002-4937-1836

Justin V. Strauss https://orcid.org/0000-0003-3298-3227

REFERENCES

- Braathen, A., Osmundsen, P. T., Maher, H., & Ganerød, M. (2018). The Keisarhjelmen detachment records Silurian-Devonian extensional collapse in Northern Svalbard. *Terra Nova*, 30, 34–39.
- Colpron, M., & Nelson, J. L. (2009). A Paleozoic northwest passage: Incursion of Caledonian, Baltican and Siberian terranes into eastern Panthalassa, and the early evolution of the North American Cordillera. Geological Society London Special Publications, 318, 273-307.
- Czerny, J., Kieres, A., Manecki, M., & Rajchel, J. (1993). Geological map of the SW part of Wedel Jarlsberg Land, Spitsbergen 1: 25 000. Kraków: Institute of Geology and Mineral Deposits.
- Dallmann, W. K., Elvevold, S., Majka, J., & Piepjohn, K. (2015). Chap. 8: Tectonics and tectonothermal events. In W. K. Dallmann (Ed.), Geoscience Atlas of Svalbard. Norsk Polarinst Rapportserie 148, 175–220.
- Dallmeyer, R. D. (1989). Partial thermal resetting of ⁴⁰Ar/³⁹Ar mineral ages in western Spitsbergen, Svalbard: Possible evidence for Tertiary metamorphism. *Geological Magazine*, 126, 587–593.
- Dallmeyer, R., Peucat, J. J., Hirajima, T., & Ohta, Y. (1990). Tectonothermal chronology within a blueschist-eclogite complex, west-central Spitsbergen, Svalbard: Evidence from ⁴⁰Ar/³⁹Ar and Rb-Sr mineral ages. *Lithos*, *24*, 291–304.
- Dewey, J. F., & Strachan, R. A. (2003). Changing Silurian-Devonian relative plate motion in the Caledonides: Sinistral transpression to sinistral transtension. *Journal of the Geological Society*, 160, 219-229
- Dodson, M. H. (1973). Closure temperature in cooling geochronological and petrological systems. Contributions to Mineralogy and Petrology, 40, 259–274.
- Dunlap, W. J. J. (1997). Neocrystallization or cooling? ⁴⁰Ar/³⁹Ar ages of white micas from low-grade mylonites. *Chemical Geology*, 143, 181–203.
- Friend, P. F., Harland, W. B., Rogers, D. A., Snape, I., & Thornley, R. S. W. (1997). Late Silurian and Early Devonian stratigraphy and probable strike-slip tectonics in northwestern Spitsbergen. *Geological Magazine*, 134, 459-479.
- Gasser, D., & Andresen, A. (2013). Caledonian terrane amalgamation in Svalbard: Detrital zircon provenance of Mesoproterozoic to Carboniferous strata from Oscar II Land, western Spitsbergen. Geological Magazine, 6, 1103–1126.
- Gee, D. G. (1975). A tectonic model for the central part of the Scandinavian Caledonides. *American Journal of Science*, 275(A), 468–515.
- Gee, D. G., Majka, J., Janák, M., Robinson, P., & van Roermund, H. (2013). Subduction along and within the Baltoscandian margin during closing of the lapetus Ocean and Baltica-Laurentia collision. *Lithosphere*, 5, 169–178.
- Gee, D. G., & Moody-Stuart, M. (1966). The base of the Old Red Sandstone in central north Haakon VII Land, Vestspitsbergen. Norsk Polarinstitutt Årbok, 1964, 57–68.
- Gee, D. G., & Page, L. M. (1994). Caledonian Terrane assembly on Svalbard – new evidence from ⁴⁰Ar/³⁹Ar dating in Ny Friesland. American Journal of Science, 294, 1166–1186.
- Gee, D. G., & Tebenkov, M. (2004). Svalbard: A fragment of the Laurentian margin. *Geological Society, London, Memoirs*, 30, 191–206.
- Harland, W. B. (1997). The Geology of Svalbard. *Geological Society*, London, Memoirs, 17, 16-44.
- Harland, W. B., Cutbill, J. L., Friend, P. F., Gobbett, D. J., Holliday, D. W., Maton, P. I., ... Wallis, R. H. (1974). The Billefjorden fault zone, Spitsbergen: The long history of a major tectonic lineament. Norsk Polarinstitutt Tiddskrifter, 161, 1–72.
- Harland, W. B., Scott, R. A., Aukland, K. A., & Snape, I. (1992). The Ny Friesland Orogen, Spitsbergen. Geological Magazine, 129, 679-708.

- Harland, W. B., & Wright, N. J. R. (1979). Alternative hypothesis for the pre-Carboniferous evolution of Svalbard. Norsk Polarinstitutt Tiddskrifter, 167, 89-117.
- Harrison, T. M., Célérier, J., Aikman, A. B., Hermann, J., & Heizler, M. T. (2009). Diffusion of ⁴⁰Ar in muscovite. *Geochimica et Cosmochimica Acta*, 73, 1039–1051.
- Johansson, Å., Gee, D. G., Björklund, L., & Witt-Nilsson, P. (1995). Isotope studies of granitoids from the Bangenhuk Formation, Ny Friesland Caledonides, Svalbard. Geological Magazine, 132, 303-320.
- Labrousse, L., Elvevold, S., Lepvrier, C., & Agard, P. (2008). Structural analysis of high-pressure metamorphic rocks of Svalbard: Reconstructing the early stages of the Caledonian orogeny. *Tectonics*, 27, 22.
- Lanari, P., Vidal, O., De Andrade, V., Dubacq, B., Lewin, E., Grosch, E. G., & Schwartz, S. (2014). XMapTools: A MATLAB-based program for electron microprobe X-ray image processing and geothermobarometry. Computers and Geosciences, 62, 227–240.
- Majka, J., Be'eri-Shlevin, Y., Gee, D. G., Czerny, J., Frei, D., & Ladenberger, A. (2014). Torellian (c. 640 Ma) metamorphic overprint of Tonian (c. 950 Ma) basement in the Caledonides of southwestern Svalbard. Geological Magazine, 151, 732-748.
- Majka, J., & Kośmińska, K. (2017). Magmatic and metamorphic events recorded within the Southwestern Basement Province of Svalbard. Arktos. 3. 5.
- Majka, J., Kośmińska, K., Mazur, S., Czerny, J., Piepjohn, K., Dwornik, M., & Manecki, M. (2015). Two garnet growth events in polymetamorphic rocks in southwest Spitsbergen, Norway: Insight in the history of Neoproterozoic and early Paleozoic metamorphism in the High Arctic. Canadian Journal of Earth Sciences, 52, 1–17.
- Majka, J., Mazur, S., Manecki, M., Czerny, J., & Holm, D. K. (2008). Late Neoproterozoic amphibolite-facies metamorphism of a pre-Caledonian basement block in southwest Wedel Jarlsberg Land, Spitsbergen: New evidence from U-Th-Pb dating of monazite. Geological Magazine, 145(6), 822-830.
- Mancktelow, N. S., & Pennacchioni, G. (2004). The influence of grain boundary fluids on the microstructure of quartz-feldspar mylonites. *Journal of Structural Geology*, 26, 47–69.
- Manecki, M., Holm, D. K., Czerny, J., & Lux, D. (1998). Thermochronological evidence for late Proterozoic (Vendian) cooling in southwest Wedel Jarlsberg Land, Spitsbergen. *Geological Magazine*, 135, 63–69.
- Mazur, S., Czerny, J., Majka, J., Manecki, M., Holm, D., Smyrak, A., & Wypych, A. (2009). A strike-slip terrane boundary in Wedel Jarlsberg Land, Svalbard, and its bearing on correlations of SW Spitsbergen with the Pearya terrane and Timanide belt. *Journal of the Geological Society*, 166, 529–544.
- McCann, A. J. (2000). Deformation of the Old Red Sandstone of NW Spitsbergen; links to the Ellesmerian and Caledonian orogenies. Geological Society, London, Special Publications, 180, 567–584.
- McClelland, W. C., Malone, S. J., von Gosen, W., Piepjohn, K., & Laeufer, A. (2012). The timing of sinistral displacement of the Pearya Terrane along the Canadian Arctic Margin. Zeitschrift Der Deutschen Gesellschaft Fur Geowissenschaften, 163, 251–259.
- McClelland, W. C., Von Gosen, W., & Piepjohn, K. (2019). Tonian and Silurian magmatism in Nordaustlandet: Svalbard's place in the Caledonian orogen. In K. Piepjohn, J. V. Strauss, L. Reinhardt, & W. C. McClelland (Eds.), Circum-Arctic Structural Events: Tectonic Evolution of the Arctic Margins and Trans-Arctic Links with Adjacent Orogens. Geological Society of America Special Papers, 541, 63–80.
- Michalski, K., Lewandowski, M., & Manby, G. (2012). New palaeomagnetic, petrographic and ⁴⁰Ar/³⁹Ar data to test palaeogeographic reconstructions of Caledonide Svalbard. *Geological Magazine*, 149, 696–721.

- Michalski, K., Manby, G., Nejbert, K., Domańska-Siuda, J., & Burzyński, M. (2017). Using palaeomagnetic and isotopic data to investigate late to post-Caledonian tectonothermal processes within the Western Terrane of Svalbard. *Journal of the Geological Society*, 174, 572-590.
- Miller, E. L., Kuznetsov, N., Soboleva, A., Udoratina, O., Grove, M. J., & Gehrels, G. (2011). Baltica in the Cordillera? *Geology*, 39, 791–794.
- Molnar, P., & Tapponnier, P. (1975). Cenozoic tectonics of Asia: Effects of a continental collision. *Science*, 189, 419–426.
- Mulch, A., & Cosca, M. A. (2004). Recrystallization or cooling ages: In situ UV-laser ⁴⁰Ar/³⁹Ar geochronology of muscovite in mylonitic rocks. *Journal of the Geological Society*, *161*, 573–582.
- Ohta, Y. (1994). Caledonian and Precambrian history in Svalbard: A review, and an implication of escape tectonics. *Tectonophysics*, 231, 183–194.
- Ohta, Y., Dallmeyer, R. D., & Peucat, J. J. (1989). Caledonian terranes in Svalbard. In R. D. Dallmeyer (Ed.), Terranes in the Circum-Atlantic Paleozoic Orogens. Geological Society of America Special Paper, 230, 1–15.
- Parra, T., Vidal, O., & Agard, P. (2002). A thermodynamic model for Fe-Mg dioctahedral K white micas using data from phase-equilibrium experiments and natural pelitic assemblages. *Contributions to Mineralogy and Petrology*, 143, 706–732.
- Pease, V. (2011). Eurasian orogens and Arctic tectonics: An overview. Geological Society, London, Memoirs, 35, 311–324.
- Schneider, D. A., Faehnrich, K., Majka, J., & Manecki, M. (2019). ⁴⁰Ar/³⁹Ar geochronologic evidence of Eurekan deformation within the West Spitsbergen Fold and Thrust Belt. In K. Piepjohn, J. V. Strauss, L. Reinhardt, & W. C. McClelland (Eds.), Circum-arctic structural events: Tectonic evolution of the Arctic margins and trans-Arctic links with adjacent orogens. Geological Society of America Special Papers, 541, 153–168.
- Soper, N. J., Strachan, R. A., Holdsworth, R. E., Gayer, R. A., & Greiling, R. O. (1992). Sinistral transpression and the Silurian closure of lapetus. Journal of the Geological Society, 149, 871–880.
- Stipp, M., Stünitz, H., Heilbronner, R., & Schmid, S. M. (2002). The eastern Tonale fault zone: A 'natural laboratory' for crystal plastic deformation of quartz over a temperature range from 250 to 700°C. Journal of Structural Geology, 24, 1861–1884.
- Strauss, J. V., Hoiland, C. W., Ward, W. P., Johnson, B. G., Nelson, L. L., & McClelland, W. C. (2017). Orogen transplant: Taconic-Caledonian arc magmatism in the central Brooks Range of Alaska. Bulletin of the Geological Society of America, 129, 649–676.
- Strauss, J. V., Macdonald, F. A., Taylor, J. F., Repetski, J. E., & McClelland, W. C. (2013). Laurentian origin for the North Slope of Alaska: Implications for the tectonic evolution of the Arctic. *Lithosphere*, 477–482.
- Tapponnier, P., Peltzer, G., Le Dain, A. Y., Armijo, R., & Cobbold, P. (1982). Propagating extrusion tectonics in Asia: New insights from simple experiments with plasticine. *Geology*, 10, 611–616.
- Teyssier, C., Tikoff, B., & Markley, M. (1995). Oblique plate motion and continental tectonics. *Geology*, 23(5), 447–450.
- Urai, J. L., Means, W. D., & Lister, G. S. (1986). Dynamic recrystallization of minerals. In B. E. Hobbs, & H. C. Heard (Eds.), Mineral and rock deformation: Laboratory studies. Geophysical Monograph, 36, 141, 190.
- Vidal, J. L., Kubin, L., Debat, P., & Soula, J. C. (1980). Deformation and dynamic recrystallization of K feldspar augen in orthogneiss from Montagne Noire, Occitania, southern France. *Lithos*, 13(3), 247–255.
- Woodcock, N. H. (1986). The role of strike-slip fault systems at plate boundaries. *Philosophical Transactions of the Royal Society of London*. Series A, Mathematical and Physical Sciences, 317(1539), 13–29.

SUPPORTING INFORMATION

Additional supporting information may be found online in the Supporting Information section.

Data S1. Analytical methods and extended discussion of results.

Table S1. Electron microprobe point analyses on white mica, samples from Wedel Jarlsberg Land, Svalbard.

Table S2. Total fusion $^{40}\text{Ar}/^{39}\text{Ar}$ data of white mica from Wedel Jarlsberg Land, Svalbard.

How to cite this article: Faehnrich K, Majka J, Schneider D, et al. Geochronological constraints on Caledonian strike-slip displacement in Svalbard, with implications for the evolution of the Arctic. *Terra Nova*. 2020;32:290–299. https://doi.org/10.1111/ter.12461